



Combining SPOT Synthesis and Native Peptide Ligation to Create Large Arrays of WW Protein Domains**

Florian Toepert, Tobias Knaute, Stefan Guffler,
José R. Pirés, Thorsten Matzdorf, Hartmut Oschkinat,
and Jens Schneider-Mergener*

Screening libraries of recombinantly expressed proteins and peptides is a common method to identify ligands with desired binding properties. Recent advances in protein synthesis, however, provide a basis for the chemical generation of large arrays of synthetic proteins that represent an alternative to recombinant technology. Novel synthetic procedures allow the chemoselective coupling of unprotected protein fragments, which can be produced synthetically or by recombinant expression (semi-synthesis).^[1–8] The chemical synthesis of proteins allows the direct introduction of several post-translational modifications and a number of nonproteinogenic residues. Here we report on the identification of variants of the human Yes-kinase associated protein (hYAP) WW protein domain with novel binding specificities within an array of 11 859 synthetic variants of the WW domain.

WW domains have a length of about 40 amino acids. They mediate protein–protein interactions in the cell and were shown to be important in numerous diseases, such as Liddle's syndrome, muscular dystrophy, Alzheimer's disease, chorea Huntington, and cancer.^[9,10] WW domains are also important model proteins for studying β -sheet motifs.^[11] The hYAP WW domain binds to proline-rich sequence motifs PPxY (x = L-amino acid).^[10] Substituting or phosphorylating tyrosine (Y) in the PPxY motif disrupts binding to the hYAP WW domain. The three-dimensional structure of the complex formed between the hYAP WW domain and the ligand shows the amino acids located at the binding interface (Figure 1 a).^[12] The essential tyrosine residue from the peptide ligand points into a binding groove composed of L30, H32, and Q35, which suggests that these three residues are key determinants for tyrosine recognition (the residues are numbered according to ref. [13]). These positions were selected for substitution to alter the binding specificity of the hYAP WW domain.

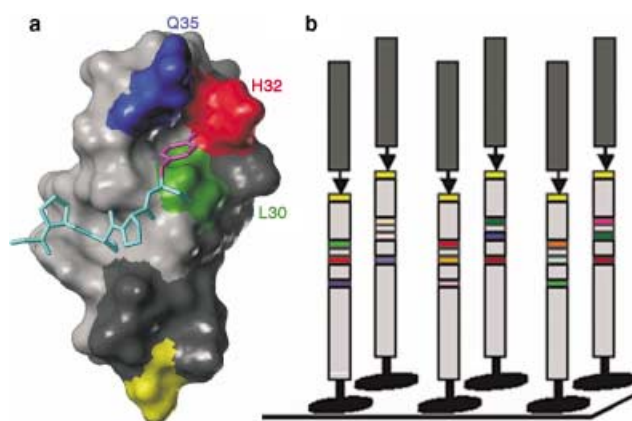


Figure 1. a) Model of the hYAP WW domain complexed with peptide ligand GPPPY.^[12] The tyrosine residue (magenta) of the peptide ligand (light blue) interacts with residues L30 (green), H32 (red), and Q35 (dark blue) of the WW domain. The ligation site at position 24^[17] is yellow. b) Synthesis strategy: Variants of the C-terminal fragment (residues 24–47, light gray) carrying an N-terminal cysteine for ligation (yellow) were prepared by stepwise SPOT synthesis^[14–16] in an array format on a cellulose membrane (NH₂-C²⁴GQRY(X¹⁴)RKAML⁴⁷-membrane). Positions 30, 32, and 35 were varied systematically (colored). The N-terminal fragment (residues 10–23, NH₂-D¹⁰VPLPAGWE-MAKTS²³-COSR), dark gray) was coupled to the C-terminal fragments by native chemical ligation^[1,3,7] to yield full-length membrane-bound WW domains.

The combination of SPOT synthesis^[14–16] and native chemical peptide ligation^[1,3,7] (Figure 1 b) enabled us to synthesize large arrays of hYAP WW domain variants (38 mers) comprising the complete set of simultaneous substitutions of positions 30, 32, and 35 against any of the 19 proteinogenic L-amino acids, excluding cysteine. This process resulted in $19^3 = 6859$ different variants (array 1). A further 5000 variants were synthesized bearing combinations of amino acids from an expanded set of residues (19 L-amino acids and 20 nonproteinogenic and phosphorylated amino acids) in positions 30, 32, and 35 (array 2). Position 24 had been identified as a suitable ligation site in a previous study.^[17] The identity of the wild-type WW domain synthesized on the cellulose membrane was confirmed by mass spectrometry (not shown).

Incubating arrays 1 and 2 with dye-labeled peptide ligand GTPPPPYTVG (Y-pep) resulted in strong signals from the 26 wild-type-containing spots at the bottom of each spot block, thus demonstrating the presence of functional WW domains on the cellulose membrane (Figure 2, underlined). The other spots resulted in signals with a wide range of intensities. To facilitate interpretation of these data the signal intensities obtained from array 1 were represented in a compact three-dimensional diagram (cube plot; Figure 3 a).

Cubes in the diagram represent WW variants that yield signal intensities that are significantly higher than the average of all the signals (see methods). The red cube in the foreground of Figure 3 a represents WW variant I30, H32, M35 (IHM), which is a strong binder to peptide ligand GTPPPPYTVG (Table 1). The cube marked by a white circle represents the hYAP WW wild-type (L30, H32, Q35; average

[*] Prof. Dr. J. Schneider-Mergener, Dr. F. Toepert, Dipl.-Chem. T. Knaute
Institut für Medizinische Immunologie
Charité, Humboldt-Universität Berlin
Hessische Strasse 3-4, 10115 Berlin (Germany)
Fax: (+49) 030-450-524-942
E-mail: jsm@charite.de

Dr. J. R. Pirés, T. Matzdorf, Prof. Dr. H. Oschkinat
Forschungsinstitut für Molekulare Pharmakologie
Robert-Rössle-Strasse 10, 13125 Berlin (Germany)
Prof. Dr. J. Schneider-Mergener, S. Guffler
Jerini AG
Invalidenstrasse 130, 10115 Berlin (Germany)

[**] This work was supported by the DFG, Universitätsklinikum Charité Berlin, and the Fonds der Chemischen Industrie.

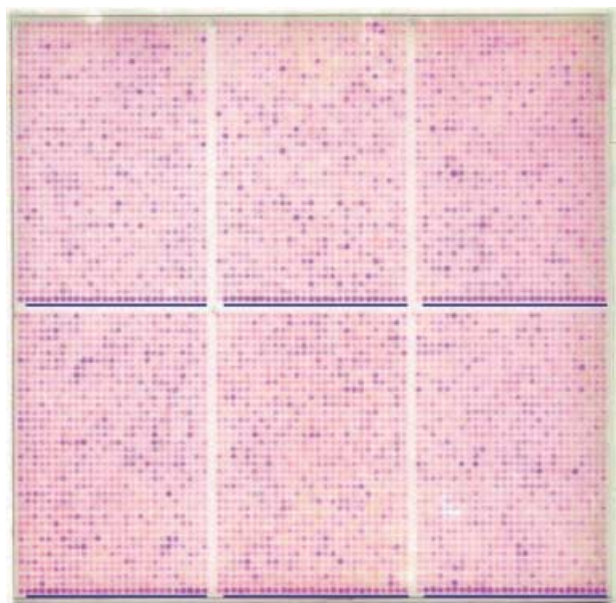


Figure 2. Interaction of peptide ligand TMR-GTPPPPYTVG with an array of WW domain variants (TMR = tetramethylrhodamine). Each spot comprises a WW variant with positions 30, 32, and 35 substituted by one of 19 L-amino acids (cysteine excluded). All possible $19^3 = 6859$ variants containing L-amino acids were synthesized (6000 shown). 26 spots at the bottom of each spot block contain the WW wild-type domain as a positive control (underlined).

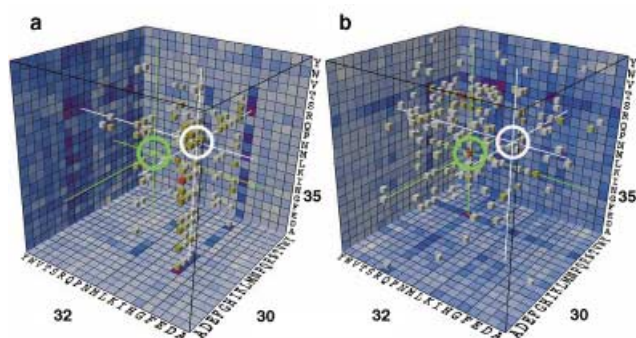


Figure 3. Cube plots displaying the binding data obtained from the interaction of peptide ligands GTPPPPYTVG (a) and GTPPPPyTVG (b) with the array of WW domains. Cubes in the diagram represent WW variants of the array that yield signal intensities that are significantly higher than the average of all signal intensities (red = highest values). The position of a cube in the diagram reflects the amino acid substitutions at positions 30, 32, and 35. The background tiles mirror the average signal intensity of the spots corresponding to the 19 cubes perpendicular to the tile (red = highest values).

of the signals from the wild-type-containing spots). The clustering of cubes in Figure 3a reveals there are similarities in the sequences of WW variants that bind Y-pep. A distinct cluster of cubes represents WW variants that contain histidine at position 32. Less prominent accumulations of cubes can be identified that represent WW variants containing N32, I30, K30, L30, M30, V30, G35, K35, M35, Q35, and R35. Previous binding studies with single-substitution variants of the hYAP WW domain corroborate the requirement for histidine or

asparagine in position 32 and the less stringent prerequisites for positions 30 (I, L, M, V) and 35 (A, G, H, K, M, Q, R).^[17]

Having identified WW variants that bind Y-pep we searched for WW variants that bind other peptide ligands. Twenty-one dye-labeled peptide ligands GTPPPPxTVG (x-pep; x = L-amino acid excluding cysteine and tyrosine but including phosphoserine (pS), phosphothreonine (pT), and phosphotyrosine (pY)) were incubated with both arrays successively and the signal intensities obtained from array 1 were represented in cube plots. Figure 3b shows the cube plot obtained for peptide ligand GTPPPPyTVG (pY-pep). The different clustering of cubes in the two plots (Figure 3) reflects a fundamental change of amino acid requirements at positions 30, 32, and 35 of the WW domain upon phosphorylation of the tyrosine residue in the peptide ligand. As expected, the wild-type domain does not bind pY-pep (white circle in Figure 3b—no cube). There are, however, several WW variants that interact significantly with pY-pep, as represented by the cubes in Figure 3b. The variant showing the highest signal intensity for pY-pep interaction has amino acids R, R, and K in positions 30, 32, and 35, respectively (RRK; green circle in Figure 3b—red cube). However, this RRK variant does not bind to wild-type ligand Y-pep, thus indicating that the wild-type WW domain and WW variant RRK have distinct binding specificities (green circle in Figure 3a—no cube).

Selected WW variants were synthesized by standard methods and their affinities towards different peptide ligands were measured by surface plasmon resonance spectroscopy (SPR; Table 1). The affinities that were detected are in the same range as the wild-type interaction (hYAP WW wild-type for Y-pep, $K_D = 94 \mu\text{M}$) and, in accordance with previous studies, we find a good correlation between binding affinities and the signal intensities obtained in array-based binding experiments (Table 1).^[17]

As in WW variant RRK, a cluster of basic residues is frequently found in proteins that bind phosphate groups,^[18] which suggests that polar interactions contribute significantly to the binding affinity. WW variant RRK, however, has a much higher affinity towards pY-pep as compared to variant

Table 1: Binding constants and signal intensities of complexes formed between the WW domain and the ligand.

| WW variant ^[a] | Peptide ligand ^[b] | K_D [μM] ^[c] | Signal intensity |
|---------------------------|-------------------------------|--|------------------|
| LHQ (wt) | Y-pep (wt) | 94 ± 18 | 100 |
| IHM | Y-pep (wt) | 68 ± 13 | 147 |
| RRK | Y-pep (wt) | nb | < 1 |
| RRR | Y-pep (wt) | nb | 3 |
| LHQ (wt) | pY-pep | nb | 3 |
| IHM | pY-pep | nb | < 1 |
| RRK | pY-pep | 40 ± 8 | 141 |
| RRR | pY-pep | 174 ± 33 | 75 |

[a] WW variants (left column) are denoted according to their substitutions at positions 30, 32, and 35 (LHQ = wt). Peptide ligands x-pep (central column) are denoted according to the amino acid (x) in the 7'-position (GTPPPPxTVG). None of the WW variants examined binds peptide ligands pS-pep or pT-pep. [b] wt = wild-type. [c] Binding constants (K_D) were determined by SPR. nb = no binding detected.

RRR (Table 1). Moreover WW variant RRK does not bind pS-pep (GTPPPPpSTVG) or pT-pep (GTPPPPpTTVG), which indicates that the phosphate moiety has to be presented in a specific structural context to permit binding of the ligand.

The three-dimensional structure of WW variant RRK complexed with pY-pep was determined by NMR spectroscopy (Figure 4a) and compared to the structure of the wild-

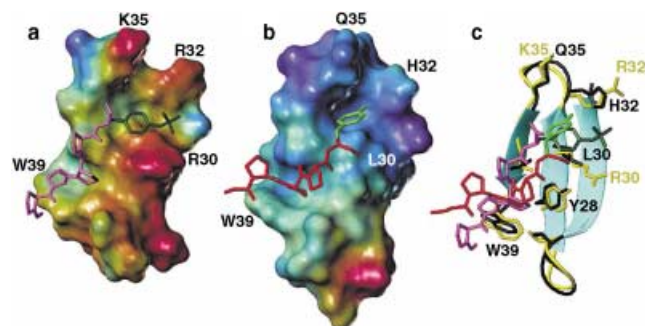


Figure 4. Comparison of three-dimensional structures of hYAP WW wild-type and variant RRK in complex with peptide ligands. Protein surfaces are colored by electrostatic potential; red indicates a positive and blue a negative potential. Peptide ligands are truncated for visual clarity. a) Three-dimensional structure of hYAP WW variant R30, R32, K35 (RRK) in the complex with peptide ligand GTPPPPpYTVG determined by NMR spectroscopy. b) Three-dimensional structure of hYAP WW wild-type complexed with peptide ligand GPPPPY.^[12] c) Ribbon representation of both complexes superimposed by matching the α -carbon atoms of residues 28, 30, 32, 35, 37, and 39.

type hYAP WW domain complexed with the unphosphorylated peptide ligand GPPPPY^[12] (Figure 4b). Both structures are superimposed in Figure 4c. The configuration of the peptide ligands is slightly different in these complexes but a number of hydrophobic contacts (seven intermolecular NOE interactions) and two intermolecular hydrogen bonds present in both complexes demonstrate that the overall orientation of the ligands is the same. The altered configuration of the peptide ligand in the RRK complex enhances electrostatic and possibly H-bonding interactions of the phosphotyrosine moiety with R30 and R32 (supported by five intermolecular NOE interactions).

Until now no naturally occurring phosphotyrosine-specific WW domains have been reported. Furthermore, searching a database of WW domains identified by sequence homology did not reveal any naturally occurring WW domains carrying amino acid substitutions R, R, and K in the sequence positions equivalent to positions 30, 32, and 35 of the hYAP WW domain. Thus, this result suggests that if phosphotyrosine-specific WW domains are present in the cell, then amino acids different from the positions that were varied in this study contribute essential contacts to the phosphotyrosine residue of the ligand.

Incubation of F-pep (GTPPPPFTVG) with array 1 resulted in a cube-plot profile (not shown) that was significantly different from that for the structurally similar Y-pep (Figure 3a). This result indicates the high sensitivity of the interaction between the WW domain and the ligand towards

small structural changes. Maximum signal intensities were lower in this experiment though, and we did not identify a specific binder to F-pep in subsequent conventional binding studies using SPR.

Cube plots obtained from incubations with Y-pep, pY-pep, F-pep, W-pep, L-pep, K-pep, and R-pep were found to display distinct clusters of cubes that indicated the presence of specific interactions. We did not identify specific binders to W-pep, L-pep, K-pep, or R-pep in subsequent conventional binding studies using SPR, however.

Cube plots obtained from incubations with the remaining peptide ligands (GTPPPPpTVG) displayed either no strong interactions at all or strong interactions between peptide ligands and WW variants containing at least two aromatic amino acids in the variable positions. These interactions can probably be attributed to nonspecific interactions of aromatic amino acids with the proline residues that are present in all of the ligands. However, the library versus library approach presented in this study provided us with the opportunity to compare the results from binding experiments with different peptide ligands, thus enabling us to distinguish specific and nonspecific interactions in a straightforward manner.

The study presented here shows that a combination of SPOT synthesis and native chemical peptide ligation can be used to generate large arrays of variants of a protein domain. The novel approach significantly expands the size-range of polypeptides that is accessible in an array format. Synthesis of an array of more than 10000 variants of the WW protein domain and screening with 22 different peptide ligands successively facilitated the observation and documentation of more than 250000 binding experiments, and revealed comprehensive information regarding the sequence requirements for binding (cube plots). Furthermore, the library versus library approach presented here allows a facile distinction between specific and nonspecific interactions. The discovery of a WW domain variant with novel binding specificity presented in this study makes synthetic protein arrays a promising new tool for the identification of tailor-made specific binders. Advances in automation and protein chemistry will promote the development of even larger arrays of synthetic proteins with an extended range of applications. Since the synthetic generation of proteins allows the facile and defined introduction of posttranslational modifications frequently involved in the regulation of protein interactions,^[19–22] arrays of synthetic protein domains may also become a valuable complement to existing methods for examining the network of cellular protein interactions.

Experimental Section

Synthesis of peptide ligands and soluble WW variants for binding studies: Syntheses were carried out according to standard protocols by using 9-fluorenylmethoxycarbonyl (Fmoc) chemistry with an automated peptide synthesizer (Intavis Bioanalytical Instruments AG, Bergisch Gladbach, Germany). Products were purified using HPLC and analyzed by MALDI-TOF mass spectrometry.

Synthesis of WW domain arrays: A library of different WW C-termini containing an N-terminal cysteine for ligation was produced by semi-automatic SPOT synthesis (Intavis Bioanalytical Instru-

ments AG, Bergisch Gladbach, Germany; software LISA (Jerini AG, Berlin, Germany)) on Whatman 50 cellulose membranes.^[14–16] Non-proteinogenic amino acids were coupled with one equivalent of 1-ethoxycarbonyl-2-ethoxy-1,2-dihydroquinoline (EEDQ) in DMF (0.3 M). The following nonproteinogenic residues were used: L-biphenylalanine, L-(2-naphthyl)alanine, L-phenylglycine, aminocyclopropionic acid, L-(2-thienyl)alanine, L-(3-pyridyl)alanine, L-citrulline, L-homoserine, L-homophenylalanine, L-(4-nitrophenyl)alanine, L-(4-guanidino)phenylalanine, L-(3,3-diphenyl)alanine, L-(2,3-diamino)propionic acid, L-(2,4-diamino)butanoic acid, L-ornithine, L-cyclohexylglycine, L-phosphoserine, L-phosphothreonine, L-phosphotyrosine, N-[3,4,6-tri-O-acetyl-2-(acetylamino)-deoxy-2-β-glucopyranosyl]-L-asparagine. The N-terminal fragment (uniform for all WW variants) containing a C-terminal thioester for ligation was synthesized as described.^[3] Ligation was achieved by dissolving the N-terminal fragment (15 mM) in ligation buffer (0.4 M sodium phosphate, pH 7.5, saturated with *p*-acetamidothiophenol) followed by incubation with the array of C-terminal fragments for 24 h. Ligation of the N-terminal WW fragment to a cellulose-bound peptide was found to proceed in 2 h with good yield. No starting material could be detected after 16 h.

Analysis of cellulose-bound wild-type hYAP WW domains: Ten spots (ca. 3 nmol peptide per spot) were punched out of the cellulose membrane. The peptides bound to the solid phase through an ester linkage were cleaved off by treatment with gaseous NH₃ for 16 h. The peptide was then eluted from the membrane with H₂O/trifluoroacetic acid (0.5%) and analyzed by HPLC-MS (system: Hewlett Packard series 1100 coupled with a Finnigan LCQ Ion Trap ESI mass spectrometer; column: Vydac C18, 150 × 2.1 mm, 300 Å, 5 μm; flow rate: 0.3 mL min⁻¹; gradient: 5–95% (acetonitrile in 0.05% aqueous TFA) in 17 min). The desired product had a retention time of 10.1 min.

Labeling of peptide ligands: Peptide ligands CββGTTPPPxTVG (x = L-amino acid, including pS, pT, pY; β = β-alanine) were linked to maleimide-activated tetramethylrhodamine (TMR, Molecular Probes, Eugene, OR, USA) through the cysteine residue according to the supplier's instructions. Remaining maleimido groups were deactivated with a tenfold excess of ethanethiol (1 h, RT), followed by purification by HPLC.

Incubation of the membrane and data acquisition: WW arrays were incubated in blocking Tris-buffered saline (TBS; 10% blocking reagent (CRB, Norwich, UK), 1% sucrose in TBS; TBS: 50 mM tris(hydroxymethyl)aminoethane (Tris), 100 mM NaCl, pH 8.0) for 1 h. Labeled peptide ligand (5 μM) was then incubated with the membrane in the same buffer at 4°C for 2 h then washed three times with TBS. The resulting spot patterns were recorded with a flatbed scanner (Snapscan e40, Agfa, Mortsel, Belgium). WW arrays were regenerated by washing with DMF (4 × 20 min) followed by washing with ethanol (3 × 3 min) and drying.

Representation of the array-based binding data in cube plots: Spot patterns obtained from the incubation of peptide ligands with array 1 were analyzed densitometrically to yield primary intensity data (software: Lumi Analysis, Roche, Mannheim, Germany). Since we wanted to focus on the effect of the variable position x of the peptide ligands (GTTPPPxTVG) upon the interaction with WW variants we compensated for possible interactions with invariable parts of the peptide ligand by subtracting, for each spot, the average primary intensity obtained by the successive interaction with all 22 peptide ligands from the primary intensity obtained with a particular ligand. The resulting signal intensities were represented in cube plots. A spot in the array was represented in the cube plot when its signal intensity was larger than the lower cut-off value, which is defined as: lower cut-off = $\bar{O} + 2.58\sigma$; with \bar{O} being the average and σ the standard deviation of all calculated signal intensities obtained for a particular peptide ligand. Background tiles represent the average signal intensity of the 19 variants of the WW domain that are identical in the sequence positions defined by the tile. Cube plots were generated with the software ICM (Molsoft, California, USA).

Measuring binding affinities of WW variants to peptide ligands: Measurements were made with a BIAcoreX system in TBS buffer. Peptide ligands were immobilized on a CM5-sensorchip through the cysteine residue with the ligand–thiol method according to the supplier's instructions. The amount of immobilized ligand corresponded to a signal increase of about 400 resonance units (RU). An equivalent amount of nonbinding peptide CββGTTPPPATVG was immobilized in the reference cell by using the same procedure. Binding experiments were performed with WW variant concentrations ranging from 1 to 500 mM (8 different concentrations were applied for each experiment). Binding experiments were performed at 25°C with a flow rate of 15 μL min⁻¹. Data were evaluated with the software BIAevaluation 3.0 according to the steady-state procedure. Error bars were estimated from a set of seven measurements of WW wild-type versus peptide ligand CββGTTPPPYTVG (reference cell: CββGTTPPPATVG) using three independently prepared sensor chips.

Determining the three-dimensional structure of WW variant RRR in the complex with peptide ligand GTTPPPpYTVG: 2D-NOESY^[23] with 150 ms mixing time and 2D-TOCSY^[24] experiments with 20, 35, and 70 ms spinlock were recorded for the complex formed between the WW domain and the ligand (1.0 mM domain and twofold molar excess of ligand) and for the WW domain alone on 600 MHz DRX or 750 MHz DMX Bruker spectrometers, respectively. Experiments were carried out in 10 mM potassium phosphate buffer, pH 6, 100 mM NaCl, 0.1 mM 1,4-dithiothreitol (DTT), 0.1 mM ethylenediamine tetraacetate (EDTA), in 90% H₂O/10% D₂O, and in 100% D₂O at 15°C. Spectra were processed with XWINNMR (Bruker) and analyzed with SPARKY (T. D. Goddard, D. G. Kneller, Sparky 3, University of California, San Francisco). 139 inter-residue NOE restraints, 12 of them intermolecular were derived from the NOESY experiment and assigned to four classes of distances (2.5 Å –0.7/+0.7; 3.5 Å –1.7/+0.7; 4.5 Å –2.7/+1.0; 5.5 Å –3.7/+1.0). Ten hydrogen bonds between the strands and two intermolecular ones were included. Eight dihedral angle restraints were added to force the ligand into a PPII helix conformation ($\phi = -78^\circ$; $\psi = +149^\circ$). Structures were calculated by simulated annealing^[25] at 2000 K by using X-PLOR 3.1 (A.T. Brünger, *X-Plor 3.1: A system for X-ray crystallography and NMR*, Yale University Press, New Haven, CT, 1993) and a floating stereospecific assignment. Force constants for NOE, bond lengths, bond angles, and improper angles were 50 kcal mol⁻¹ Å⁻², 1000 kcal mol⁻¹ Å⁻², 500 kcal mol⁻¹ rad⁻², and 500 kcal mol⁻¹ rad⁻², respectively.

Received: November 6, 2002 [Z50483]

Keywords: peptides · protein arrays · protein design · protein modifications

- [1] P. E. Dawson, T. W. Muir, I. Clark-Lewis, S. B. H. Kent, *Science* **1994**, 266, 776.
- [2] L. E. Canne, S. J. Bark, S. B. H. Kent, *J. Am. Chem. Soc.* **1996**, 118, 5891.
- [3] T. M. Hackeng, J. H. Griffin, P. E. Dawson, *Proc. Natl. Acad. Sci. USA* **1999**, 96, 10068.
- [4] P. Botti, M. R. Carrasco, S. B. H. Kent, *Tetrahedron Lett.* **2001**, 42, 1831.
- [5] T. Kawakami, K. Akaji, S. Aimoto, *Org. Lett.* **2001**, 3, 1403.
- [6] J. Offer, C. N. Boddy, P. E. Dawson, *J. Am. Chem. Soc.* **2002**, 124, 4642.
- [7] P. E. Dawson, S. B. H. Kent, *Annu. Rev. Biochem.* **2000**, 69, 923.
- [8] M. Q. Xu, T. C. Evans, Jr., *Methods Enzymol.* **2001**, 24, 257.
- [9] P. Bork, M. Sudol, *Trends Biochem. Sci.* **1994**, 19, 531.
- [10] M. Sudol, T. Hunter, *Cell* **2000**, 103, 1001.
- [11] M. Jager, H. Nguyen, J. C. Crane, J. W. Kelly, M. Gruebele, *J. Mol. Biol.* **2001**, 311, 373.

- [12] J. R. Pires, F. Taha-Nejad, F. Toepert, T. Ast, U. Hoffmüller, J. Schneider-Mergener, R. Kuhne, M. J. Macias, H. Oschkinat, *J. Mol. Biol.* **2001**, 314, 1147.
- [13] M. J. Macias, M. Hyvonen, E. Baraldi, J. Schultz, M. Sudol, M. Saraste, H. Oschkinat, *Nature* **1996**, 382, 646.
- [14] R. Frank, *Tetrahedron* **1992**, 48, 9217.
- [15] A. Kramer, U. Reineke, L. Dong, B. Hoffmann, U. Hoffmüller, D. Winkler, R. Volkmer-Engert, J. Schneider-Mergener, *J. Pept. Res.* **1999**, 54, 319.
- [16] U. Reineke, R. Volkmer-Engert, J. Schneider-Mergener, *Curr. Opin. Biotechnol.* **2001**, 12, 59.
- [17] F. Toepert, J. R. Pires, C. Landgraf, H. Oschkinat, J. Schneider-Mergener, *Angew. Chem.* **2001**, 113, 922; *Angew. Chem. Int. Ed.* **2001**, 40, 897.
- [18] J. Kuriyan, D. Cowburn, *Annu. Rev. Biophys. Biomol. Struct.* **1997**, 26, 259.
- [19] P. J. Lu, X. Z. Zhou, Y. C. Liou, J. P. Noel, K. P. Lu, *J. Biol. Chem.* **2002**, 277, 2381.
- [20] D. R. Stover, P. Furet, N. B. Lydon, *J. Biol. Chem.* **1996**, 271, 12481.
- [21] M. A. Broome, T. Hunter, *Oncogene* **1997**, 14, 17.
- [22] H. Park, M. I. Wahl, D. E. Afar, C. W. Turck, D. J. Rawlings, C. Tam, A. M. Scharenberg, J. P. Kinet, O. N. Witte, *Immunity* **1996**, 4, 515.
- [23] J. Jeener, B. H. Meier, P. Bachmann, R. R. Ernst, *J. Chem. Phys.* **1979**, 71, 4546.
- [24] L. Braunschweiler, R. R. Ernst, *J. Magn. Reson.* **1983**, 53, 521.
- [25] J. Kuszewski, M. Nilges, A. T. Brunger, *J. Biomol. NMR* **1992**, 2, 33.